

# IMAGE AND SPECTRUM BASED DEEP FEATURE ANALYSIS FOR PARTICLE MATTER ESTIMATION WITH WEATHER INFORMATION

Zanbo Zhu, Ruobing Zhao, Jianyuan Ni, Jing Zhang

Computer Science Department, Lamar University, Beaumont, TX, USA

## ABSTRACT

Air pollution is a major global risk to human health and environment. Particle matter (PM) with diameters less than 2.5 micrometers ( $PM_{2.5}$ ) is more harmful to human health than other air pollutants because it can penetrate deeply into lungs and damage human respiratory system. A new image-based deep feature analysis method is presented in this paper for  $PM_{2.5}$  concentration estimation. Firstly, low level and high level features are extracted from images and their spectrums by a deep learning neural network, and then regression models are created using the extracted deep features to estimate the  $PM_{2.5}$  concentrations, which are future refined by the collected weather information. The proposed method was evaluated using a  $PM_{2.5}$  dataset with 1460 photos and the experimental results demonstrated that our method outperformed other state-of-the-art methods.

**Index Terms**— Deep Features, Particle Matter, Image, Spectrum, Weather Information

## 1. INTRODUCTION

Airborne particulate matter (PM) represents a complex mixture of solid (e.g., dust, soot, smoke) and liquid particles suspended in air. Part of the inorganic and organic components in PM is regarded hazardous and poses a threat to public health. Fine particles with aerodynamic diameters of less than 2.5  $\mu\text{m}$  ( $PM_{2.5}$ ) can penetrate deep into human's lung and even mix with bloodstream. Epidemiological studies have established the health risks of increased cardiopulmonary and lung cancer mortality through short-term/long-term exposures to these fine and coarse atmospheric particles. Recently, PM has emerged as a leading air pollutant and become more serious than ever before due to rapid global urbanization and industrialization. For example, PM pollution is estimated to cause 22,000-52,000 deaths in U.S. and 3 million deaths globally [1], and the annual mean  $PM_{2.5}$  concentration in China increased from 25.23 $\mu\text{g}/\text{m}^3$  in 1999 to 37.51 $\mu\text{g}/\text{m}^3$  in 2011 [2].

Because of the health and environmental concerns caused by PM, annual and daily  $PM_{2.5}$  concentrations have been used as metrics for ambient monitoring. Urban PM

monitoring usually measures concentration of PM at fixed stations that are set up and operated by local and national environmental agencies. However, measurements from a limited number of monitoring stations only represent PM exposure of the population in local areas where the measurements are taken. The high cost associated with setting up PM measurement devices at monitoring sites also restricts spatial resolution of continuous PM measurement. Therefore, it is crucial to develop a portable, inexpensive, reliable, and easy-to-use method for PM analysis urban and industrial areas.

Because the reduced visibility caused by  $PM_{2.5}$  air pollution can be captured by image acquisition devices (e.g., camera, infrared/ultraviolet sensor, depth sensor, etc.), analyzed by computer vision algorithms, and characterized by machine learning algorithms, many image-based  $PM_{2.5}$  estimation methods have been proposed in recent years. Liu *et al.* [3] used a support vector regression model to predict  $PM_{2.5}$  from images using six features, including dark channel prior, image contrast, image entropy, sky gradient, blue component, and sun location. Based on the dark channel prior dehazing algorithm, Li *et al.* [4] extracted the depth maps and transmission matrices from haze images and applied a logarithmic function to classify haze levels. Zhang *et al.* [5] constructed a deep neural network with nine convolution layers, two pooling layers, two dropout layers, and a negative log-log ordinal classifier to classify  $PM_{2.5}$  images into six classes. Yang *et al.* [6] proposed a  $PM_{2.5}$  index estimation (PMIE) method that uses a shallow network consisting of the first seven layers of a ResNet with layer enhancement to estimate  $PM_{2.5}$  from images. Our group has been working on image-based  $PM_{2.5}$  analysis. In our initial work [7], we applied a VGG16 deep neural network for  $PM_{2.5}$  image classification. In our subsequent study [8], we proposed the first regression method to predict  $PM_{2.5}$  using ResNet and weather features. More recently, we created an ensemble of deep neural networks [9] that uses a multilayer perceptron to combine VGG16, Inception-V3, and ResNet50 for  $PM_{2.5}$  prediction.

In this paper, we present a new method to analyze  $PM_{2.5}$  from images using the deep features extracted by deep neural network. Our contributions are: (1) the spectrums of RGB images are used for the first time in the literature for  $PM_{2.5}$  estimation; (2) low-level and high-level deep features are combined to fit  $PM_{2.5}$  estimation problem and the

features are extracted from a ImageNet pre-trained network directly without network training, which significantly reduces the running time; and (3) The proposed method outperforms other state-of-the-art methods.

## 2. MOTHEODOLOGY

The proposed method consists of four major steps: (1) generate the spectrums of the RGB images in the dataset; (2) use a deep learning network to extract low-level and high-level features from both RGB images and their spectrums; (3) apply a coarse regression to estimate  $PM_{2.5}$  concentrations based on the extracted deep features; and (4) refine the estimated  $PM_{2.5}$  concentrations using the collected weather information. The flowchart of our method is presented in Fig. 1 and the details of each step will be described in the rest of this section.

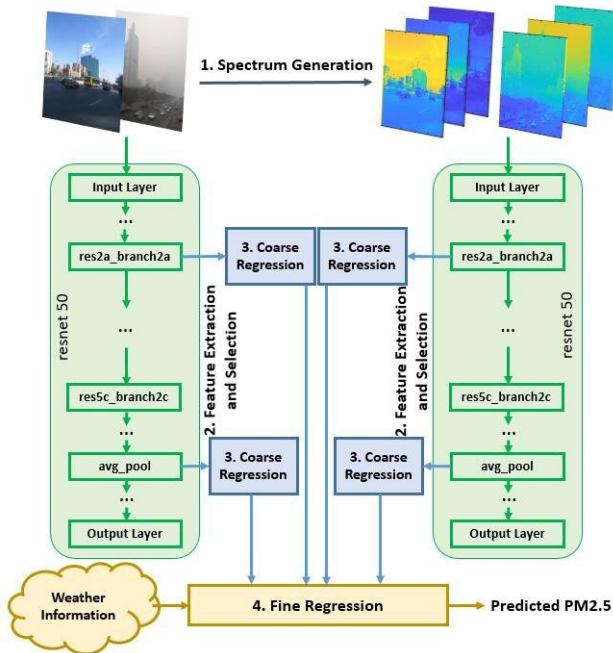


Fig. 1: Flowchart of the proposed method

### 2.1. Spectrum Generation

Scattering, the redirection of electromagnetic energy by suspended particles in the air, is a very important process in the atmosphere. Table 1 lists three main scattering types.

Table 1: Scattering types in the atmosphere

Scattering	Occurrence
Rayleigh	Particle diameter < radiation wavelength (e.g., $O_2$ , $CO_2$ )
Mie	Particle diameter $\approx$ radiation wavelength (e.g., $PM_{2.5}$ pollutants, dust)
Non-selective	Particle diameter > radiation wavelength (e.g., water droplets, fog)

When  $PM_{2.5}$  concentration is low, Rayleigh scattering occurs. Lights with shorter wavelengths (e.g., blue light) are more strongly scattered than longer wavelengths (e.g., red light). Therefore, blue spectrum is stronger than others. When  $PM_{2.5}$  concentration is high, Mie scattering occurs. Lights with longer wavelengths are more scattered and their spectrums are getting stronger compared with those of Rayleigh scattering.

Because spectrums are closely related to the presence of  $PM_{2.5}$ , spectrum information is used for the first time in the literature to estimate  $PM_{2.5}$  concentrations in this study. We adopted the approach proposed in [10] to reconstruct three spectrums with wavelengths 470nm (blue), 580nm (yellow), and 680nm (red) from RGB-only input for  $PM_{2.5}$  analysis. Fig. 2 shows two RGB images and their three spectrum images. We can see that the low  $PM_{2.5}$  image has a bigger 470nm spectrum and smaller 580nm and 680nm spectrums than the high  $PM_{2.5}$  image.

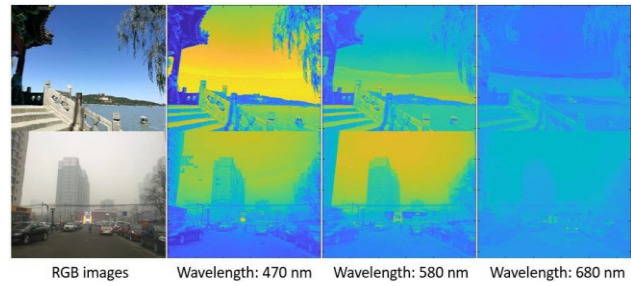


Fig. 2: Images and their spectrums.

### 2.2. Deep Feature Extraction and Selection

Estimation  $PM_{2.5}$  from images needs not only low level features, which can present edge intensities, but also high level features, which can fuse edge information with depth information to learn how the edge intensities change with the increasing depth.

Because deep neural network has an explicit end-to-end architecture and can extract both low-level and high-level features automatically, we extracted the deep features from RGB images and their spectrums as follows:

- (1) *Convolutional Neural Network (CNN)*: We compared three CNN models, VGG16, Inception-V3, and ResNet50, for  $PM_{2.5}$  prediction in our previous work [9] and found ResNet50 outperformed others. Therefore, a ResNet50 network pre-trained using ImageNet dataset was selected in this study. The images and spectrums are input to the network directly without network training to extract features.
- (2) *Low-level feature extraction*: Inspired by [6] that uses a shallow network with the first 7 blocks of a ResNet50 for  $PM_{2.5}$  analysis, we extracted the low-level features from the second convolution layer (res2a\_branch2a) in the ResNet50 model and converted the  $55 \times 55 \times 64$  dimensional features to a  $1 \times 193600$  vector.

- (3) *High-level feature extraction*: the high-level features were extracted from the average pooling layer after the last convolution layer (res5c\_branch2c), which was used as a feature extractor in several applications, such as weather classification [11], human rights violation detection [12], and parasite detection [13]. The size of the high-level features is  $1 \times 2048$ .
- (4) *Relief algorithm-based feature selection*: Due to the huge number of low-level features, a Relief feature selection [14] was applied to reduce low-level feature dimensions. Relief algorithm can penalize/reward the features that yield different values to neighboring features with the same/different response values. All features are ranked based on the calculated importance. In our study, the top ranked 2048 features were selected from the low-level image and spectrum features separately, which makes the low-level and high-level feature sets have the same number of features.

### 2.3. Coarse Regression

Four regression models are created in this step using the four extracted deep feature sets for a coarse  $PM_{2.5}$  estimation, and then the outputs will be refined by a fine regression combined with weather information in the next step to generate final estimated  $PM_{2.5}$  concentrations.

We tested different regression models, including linear regression, support vector machine (SVM) regression, and ensemble of regression trees. The predictors were 2048 features of each set and the responses were the corresponding  $PM_{2.5}$  concentrations. The linear SVM model achieved the best regression performance and was selected in our experiments.

### 2.4. Fine Regression with Weather Information

Weather features can provide very useful information to facilitate image-based  $PM_{2.5}$  analysis [9-11]. For example, fog may cause non-selective scattering that scatters most visible lights and lead to a gray sky with reduced visibility. Without humidity weather information, it is very difficult to separate foggy images and images with high  $PM_{2.5}$  concentrations by using only image features. In our study, three weather features were employed: (1) humidity: the low humidity positively affect  $PM_{2.5}$  due to accumulation effect and high humidity negatively affect  $PM_{2.5}$  due to precipitation; (2) wind speed: low wind speed can blow away the pollutants and high wind speed may bring pollutants from other emission sources; and (3) temperature: the change of temperature can affect the formation and photochemical reaction of particles.

The weather information is integrated by a fine regression step, which uses the three weather features and four coarse regression outputs as the predictors to generate the refined  $PM_{2.5}$  estimations. Ensemble of regression trees was selected for the fine regression experimentally.

## 3. EXPERIMENTAL RESULTS

In this section, we will introduce the  $PM_{2.5}$  image dataset and evaluate the performance of the proposed method.

### 3.1. $PM_{2.5}$ Image Dataset and Weather Features

The proposed method was assessed by the  $PM_{2.5}$  image dataset used in [6, 8, 9]. This dataset contains 1460 street view images captured at various locations in Beijing, China from 2013 to 2016. All images have sky regions and objects at different depths, which can provide sufficient visual information to present the air quality. The hourly  $PM_{2.5}$  historical data provided by the U.S. embassy in Beijing was used to retrieve the corresponding  $PM_{2.5}$  concentration of each image based on the photo taken time and date. The weather information of each image was collected from a weather forecast website in a similar manner. Fig. 3 illustrates the  $PM_{2.5}$  histogram of the dataset and Table 2 shows the range, mean, and standard deviation (STD) of each weather feature.

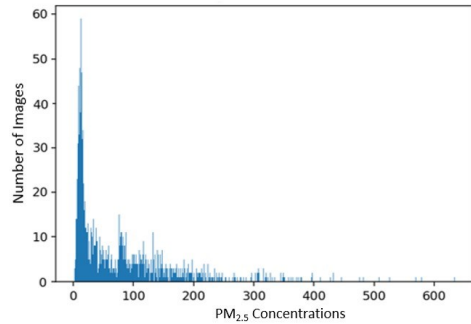


Fig. 3:  $PM_{2.5}$  histogram of Beijing dataset

Table 2: Weather Features of Beijing Dataset

	Range	Mean	STD
Humidity	6~100	40.206	22.11
Wind Speed	0~31.3	8.174	5.73
Temperature (F°)	3.2~98.6	56.542	22.23

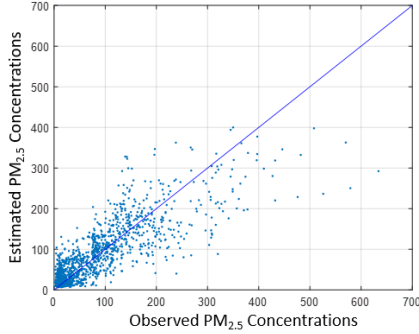
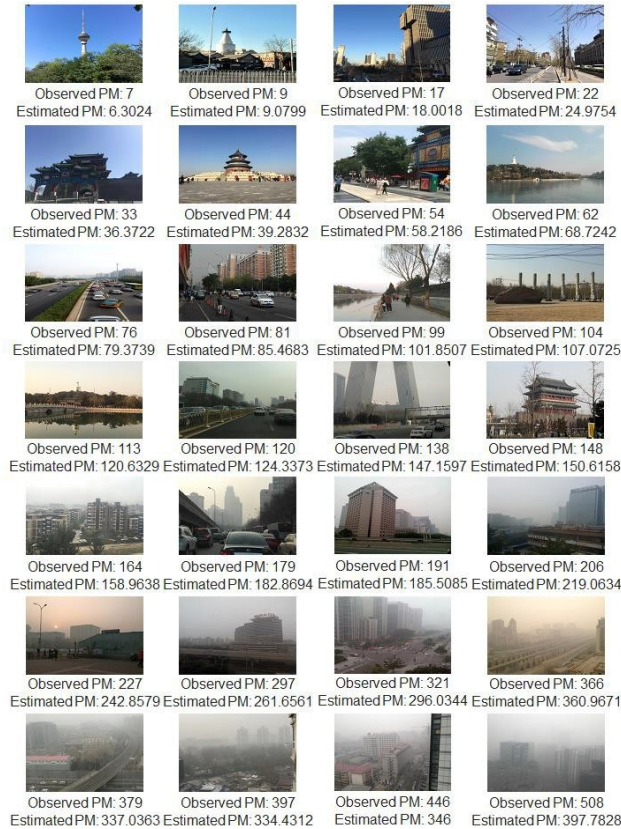
### 3.2. Performance Evaluation

The proposed method was evaluated by a 4-fold cross validation. The training dataset has 1095 images and the test dataset has 365 images. The Evaluation metrics, root mean square error (RMSE) and R-squared [15], were used for performance comparison. The program was implemented by MATLAB 2018b using a computer equipped with Intel Xeon CPU, 32 GB RAM, NVIDIA GeForce GTX 1080Ti GPU with 12 GB memory, and Ubuntu 16.04 OS.

Table 3 lists the performances of the proposed method and other state-of-the-art methods for comparison purpose. Fig. 4 shows the correlation between the estimated  $PM_{2.5}$  and observed  $PM_{2.5}$  concentrations of Beijing dataset. Some experimental results are illustrated in Fig. 5.

**Table 3: Performance Comparison**

	RMSE	$R^2$
Inception-V3 [9]	64.32	0.464
VGG-16 [9]	60.44	0.527
RseNet50 [8]	59.15	0.558
RseNet50+Weather [8]	56.03	0.605
PMIE [6]	50.64	0.680
Ensemble of CNNs [9]	49.37	0.684
<b>The proposed method</b>	<b>48.37</b>	<b>0.697</b>

**Fig. 4: Estimated  $PM_{2.5}$  vs. observed  $PM_{2.5}$** **Fig. 5: Images with observed  $PM_{2.5}$  and estimated  $PM_{2.5}$** 

### 3.3 Discussion

Table 3 shows that the proposed method achieved the best performance. It outperformed not only other single CNN-

based methods, but also the ensemble of CNNs [9] that combines three CNN models, VGG16, Inception-V3, and ResNet50, for  $PM_{2.5}$  analysis.

In order to investigate the contributions of different feature sets, we also tested the deep features extracted from images (ImgFeat), images and spectrums (ImgFeat+Spectrum), and images and spectrums with weather (ImgFeat+Spectrum+Weather). The experimental results are listed in Table 4. The spectrum features reduced RMSE by 9.9% and increased  $R^2$  by 13.3% and weather information further reduced RMSE by 5.5% and increased  $R^2$  by 5.4%, which strongly demonstrated the validity of the spectrum and weather information used in our method.

**Table 4: Performance comparison of features**

	RMSE	$R^2$
ImgFeat	56.82	0.583
ImgFeat+Spectrum	51.19	0.661
<b>ImgFeat+Spectrum+Weather</b>	<b>48.37</b>	<b>0.697</b>

Meanwhile, it is noticed that the images with high  $PM_{2.5}$  concentrations have bigger estimation errors than the images with low  $PM_{2.5}$  concentrations, as shown in Fig. 4 and the last four images in Fig. 5. This is because that the  $PM_{2.5}$  distribution of Beijing dataset is very non-uniform, as illustrated in Fig. 2. The insufficient high  $PM_{2.5}$  images may cause the regression models cannot receive enough high  $PM_{2.5}$  image and spectrum features and fail to estimate high  $PM_{2.5}$  concentrations accurately.

## 4. CONCLUSIONS

$PM_{2.5}$  is one of the most common air pollutants and may cause many severe diseases. An efficient  $PM_{2.5}$  analysis system is of great benefit for human health and air pollution control. In this paper, we propose a new image-based method to estimate  $PM_{2.5}$  concentrations. Based on the fact that spectrums are closely related to the types of particle matter in the atmosphere, spectrum information is used for the first time in the literature for  $PM_{2.5}$  analysis. The low-level and high-level deep features extracted from RGB images and their spectrums by a ResNet are combined with the weather information and fed to the regression models to estimate  $PM_{2.5}$  concentrations. The proposed method was evaluated by 1460 images and the experimental results demonstrated that our method outperformed other state-of-the-art methods. In our future work, we will investigate more spectrums with different wavelengths for  $PM_{2.5}$  analysis and collect more high  $PM_{2.5}$  images to balance the  $PM_{2.5}$  concentration distribution of the dataset.

### Acknowledgements

We gratefully acknowledge the support of NVIDIA Corporation with the donation of the GPU used for this research. The research was also partially supported by National Science Foundation under award No. 1726500.

## REFERENCES

- [1] Mokdad, Ali H., James S. Marks, Donna F. Stroup, and Julie L. Gerberding. "Actual causes of death in the United States, 2000." *Jama* 291, no. 10: 1238-1245, 2004
- [2] Li, G., Fang, C., Wang, S. and Sun, S., "The effect of economic growth, urbanization, and industrialization on fine particulate matter (PM<sub>2.5</sub>) concentrations in China" *Environmental science & technology*, 50(21), pp.11452-11459, 2016
- [3] Liu, Chenbin, Francis Tsow, Yi Zou, and Nongjian Tao. "Particle pollution estimation based on image analysis." *PLoS one* 11, no. 2 (2016): e0145955.
- [4] Li, Yuncheng, Jifei Huang, and Jiebo Luo. "Using user generated online photos to estimate and monitor air pollution in major cities." In *Proceedings of the 7th International Conference on Internet Multimedia Computing and Service*, p. 79. ACM, 2015.
- [5] Zhang, Chao, Junchi Yan, Changsheng Li, Xiaoguang Rui, Liang Liu, and Rongfang Bie. "On estimating air pollution from photos using convolutional neural network." In *Proceedings of the 2016 ACM on Multimedia Conference*, pp. 297-301. ACM, 2016.
- [6] Yang, Wenwen, Jun Feng, Qirong Bo, Yixuan Yang, and Bo Jiang. "A Shallow ResNet with Layer Enhancement for Image-Based Particle Pollution Estimation." In *Chinese Conference on Pattern Recognition and Computer Vision (PRCV)*, pp. 381-391. Springer, Cham, 2018.
- [7] Chakma, Avijoy, Ben Vizena, Tingting Cao, Jerry Lin, and Jing Zhang. "Image-based air quality analysis using deep convolutional neural network." In *Image Processing (ICIP), 2017 IEEE International Conference on*, pp. 3949-3952. IEEE, 2017.
- [8] Bo, Qirong, Wenwen Yang, Nabin Rijal, Yilin Xie, Jun Feng, and Jing Zhang. "Particle Pollution Estimation from Images Using Convolutional Neural Network and Weather Features." In *2018 25th IEEE International Conference on Image Processing (ICIP)*, pp. 3433-3437. IEEE, 2018.
- [9] Rijal, Nabin, Ravi Teja Gutta, Tingting Cao, Jerry Lin, Qirong Bo, and Jing Zhang. "Ensemble of Deep Neural Networks for Estimating Particulate Matter from Images." In *2018 IEEE 3rd International Conference on Image, Vision and Computing (ICIVC)*, pp. 733-738. IEEE, 2018.
- [10] Arad, Boaz, and Ohad Ben-Shahar. "Sparse recovery of hyperspectral signal from natural rgb images." In *European Conference on Computer Vision*, pp. 19-34. Springer, Cham, 2016.
- [11] Guerra, Jose Carlos Villarreal, Zeba Khanam, Shoaib Ehsan, Rustam Stolkin, and Klaus McDonald-Maier. "Weather Classification: A new multi-class dataset, data augmentation approach and comprehensive evaluations of Convolutional Neural Networks." In *2018 NASA/ESA Conference on Adaptive Hardware and Systems (AHS)*, pp. 305-310. IEEE, 2018.
- [12] Kalliatakis, Grigorios, Shoaib Ehsan, Maria Fasli, Ales Leonardis, Juergen Gall, and Klaus D. McDonald-Maier. "Detection of Human Rights Violations in Images: Can Convolutional Neural Networks help?." *arXiv preprint arXiv:1703.04103* (2017).
- [13] Rajaraman, Sivaramakrishnan, Sameer K. Antani, Mahdieh Poostchi, Kamolrat Silamut, Md A. Hossain, Richard J. Maude, Stefan Jaeger, and George R. Thoma. "Pre-trained convolutional neural networks as feature extractors toward improved malaria parasite detection in thin blood smear images." *PeerJ* 6 (2018): e4568.
- [14] Kononenko, Igor, Edvard Šimec, and Marko Robnik-Šikonja. "Overcoming the myopia of inductive learning algorithms with RELIEFF." *Applied Intelligence* 7, no. 1 (1997): 39-55.
- [15] Cameron, A. Colin, and Frank AG Windmeijer. "An R-squared measure of goodness of fit for some common nonlinear regression models." *Journal of econometrics* 77, no. 2 (1997): 329-342.